Kinetic Modeling of Ouabain Tissue Distribution Based on Slow and Saturable Binding to Na,K-ATPase

Hideyoshi Harashima,[1,2] Michio Mamiya,[1,3] Masayo Yamazaki,[1] Yasufumi Sawada,[1,4] Tatsuji Iga,[1,4] Manabu Hanano,[1,5] and Yuichi Sugiyama[1,6]

Received March 2, 1992; accepted June 5, 1992

The significance of the binding to Na,K-ATPase in the tissue distribution of ouabain was previously documented (Harashima *et al.*, *Pharm. Res.* 9:474–479, 1992). The purpose of this study was to obtain a kinetic model of ouabain tissue distribution. In most tissues, the ouabain concentration continued to rise after the termination of infusion (5 min), with the peak tissue concentration at approximately 20 min. This delay could not be explained by the rapid equilibrium model (RE model), nor could the kinetics of ouabain be explained by an RE model modified for saturable binding. Since ouabain binding to Na,K-ATPase is slow, the association and dissociation processes were incorporated into a model that can accurately fit the observed time courses of ouabain. The obtained binding parameters corresponded well with the observed values in the *in vitro* binding experiments, except for muscle. These results quantitatively support the role of the slow and saturable binding of ouabain to Na,K-ATPase in its tissue distribution.

KEY WORDS: cardiac glycosides; ouabain; Na,K-ATPase; guinea pig; tissue distribution; tissue-to-plasma concentration ratio; kinetic modeling.

INTRODUCTION

A physiological model of cardiac glycosides disposition was first obtained for digoxin in rat by L. I. Harrison and M. Gibaldi (1), who used a linear, flow-limited model which predicted well the tissue concentration time courses and was subsequently used for scaling up from dog to human (2). There was also a good correspondence between predicted and literature values in the elimination phase, but the distribution phase pattern of observed values differed from that of literature values. In the prediction, the tissue concentration rapidly decreases in heart, kidney, and liver, whereas the observed tissue concentrations do not change remarkably in the distribution phase. The difference is large in every tissue except muscle.

This discrepancy may stem from the invalid assumption of rapid equilibrium in the model. A slow binding process of cardiac glycosides has been shown in *in vitro* experiments (3–5). The association and dissociation processes of cardiac glycosides take place on the order of hours depending on the tissue and animal species (6,7). Rat is known to be insensitive to cardiac glycosides and the dissociation constant for cardiac Na,K-ATPase is high compared to that of dog (8). In addition, the half-life of the dissociation of cardiac glycosides from Na,K-ATPase occurs on the order of minutes in rats, while on the order of hours in dogs (8). This interspecies difference in binding of cardiac glycosides to Na,K-ATPase could be one reason for the difference in the tissue distribution as well as that in pharmacological responses.

Ouabain is known to bind Na,K-ATPase specifically, and this binding process was examined extensively *in vitro* (3). The significance of this binding in ouabain tissue distribution was shown in both rabbits and guinea pigs in our previous studies (9,10) by comparing *in vivo* ($K_{p,vivo}$) and *in vitro* ($K_{p,vitro}$) tissue to plasma concentration ratios. The $K_{p,vitro}$ derived from the binding parameters of each tissue homogenate and extracellular space agreed well with the $K_{p,vivo}$. Since the K_p represents the extent of tissue distribution in each tissue, this result indicates that ouabain tissue distribution is governed principally by its binding to Na,K-ATPase.

In this report, kinetic modeling was performed to account for the time courses of ouabain tissue distribution based on physiological and biochemical information. Ouabain was selected as a model compound because it is not bound to plasma protein, is not metabolized, and is eliminated into urine by glomerular filtration (10). The validity of the flow-limited model was first examined, then a kinetic model was developed by incorporating a slow and saturable process in the ouabain binding to and dissociation from Na,K-ATPase, using the experimental data reported previously (10).

METHODS

Experimental Data

The ouabain plasma and tissue concentration time course data for guinea pigs reported previously (10) were used. Briefly, ouabain was infused at a rate of 10 nmol/min/kg under anesthesia, and its plasma and tissue concentrations were assayed by measuring the radioactivity of ^{3}H-ouabain.

Development of the Model

The validity of the model was examined by comparing between observed and model-simulated $K_{p,vivo}$ (C_t/C_a) values, where C_t and C_a represent tissue and arterial plasma concentration of ouabain, respectively.

Rapid Equilibrium Model (RE Model). The assumption of rapid equilibrium was examined first. As shown in Fig. 1,

[1] Faculty of Pharmaceutical Sciences, University of Tokyo, Hongo, Bunkyo-ku, Tokyo 113, Japan.
[2] Present address: Faculty of Pharmaceutical Sciences, The University of Tokushima, 1-78-1 Shomachi, Tokushima 770, Japan.
[3] Present address: Shionogi and Co., Ltd. Shionogi Research Laboratories, 2-1-3 Kuise-Terashima, Amagasaki City Hyogo 660, Japan.
[4] Present address: Department of Pharmacy, University of Tokyo Hospital, Faculty of Medicine, University of Tokyo, Hongo, Bunkyo-ku, Tokyo 113, Japan.
[5] Present address: College of Pharmacy, Nihon University, 7-7-1 Narawashinodai, Funabashi City 274, Japan.
[6] To whom correspondence should be addressed.

0724-8741/92/1200-1607$06.50/0

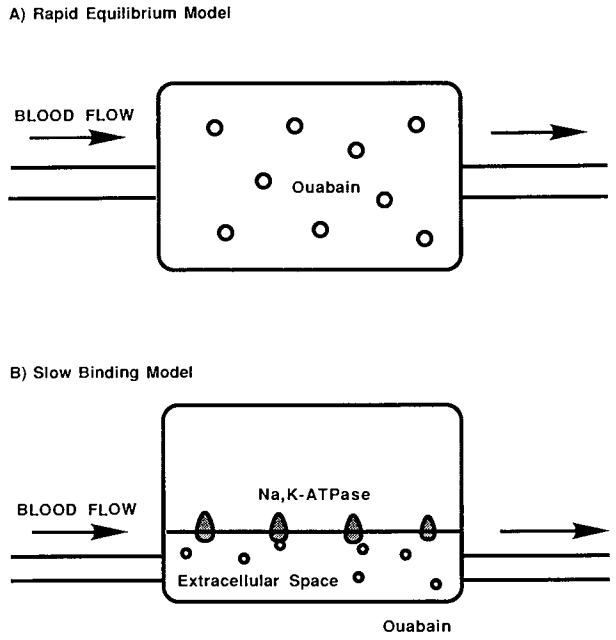

Fig. 1. Kinetic model for ouabain tissue distribution. (A) RE model: Drug is carried by plasma flow into each tissue and rapid equilibrium between tissue and venous plasma concentration is assumed and represented by K_p. (B) SB model: Drug binding to, and dissociation from, Na,K-ATPase, located in the extracellular space, is slow and represented by association and dissociation rate constants. The maximum binding capacity of Na,K-ATPase is represented by B_{max}.

this model is described by the blood flow rate (Q), tissue volume (V_t), and tissue-to-plasma concentration ratio (K_p). Since ouabain does not enter blood cells, the mass balance equation is described based on the plasma flow rate instead of the blood flow rate:

$$V_t dC_t/dt = Q(1 - Hc)(C_a - C_t/K_p) \quad (1)$$

$$K_p = C_t/C_v \quad (2)$$

where C_v represents the venous plasma concentrations of ouabain and V_t and Hc represent the tissue volume and hematocrit values, respectively. In the case of saturable binding, K_p is described as follows:

$$K_p = V_e/V_t + B_{max}/(K_d + C_v) \quad (3)$$

where V_e represents the extracellular space. B_{max} and K_d represent the maximum binding capacity and dissociation constant of ouabain for Na,K-ATPase.

Using Eq. (3), the time courses of $K_{p,vivo}$ were simulated in heart and muscle. The time course of arterial plasma concentration (C_p) was described by the following equations:

$$0 < t < 5: \quad C_p = \sum_i^3 A_i\{1 - \exp(-a_i \cdot t)\} \quad (4a)$$

$$5 < t: \quad C_p = \sum_i^3 A_i\{1 - \exp(-a_i \cdot 5)\} \exp\{-a_i(t - 5)\} \quad (4b)$$

The K_p values were fixed at 2.5 and 1.0 for heart and muscle, respectively. Equations (1)–(4b) were solved numerically by the Runge–Kutta–Gill method. For simulation, saturable binding parameters were fixed at the values obtained from *in vitro* experiments. For heart, B_{max} = 16800 (nM), and K_d = 740 (nM). For muscle, B_{max} = 155 (nM), and K_d = 1.1 (nM). Physiological parameters were obtained from the literature (10,11). For heart, V_t = 1.3 (ml), V_e/V_t = 0.123, and Q = 1.7 (ml/min). For muscle, V_t = 153 ml, V_e/V_t = 0.119, and Q = 6.3 ml/min.

Slow Binding Model (SB Model). The association rate constant (k_{on}) and dissociation rate constant (k_{off}) were incorporated to express the slow and saturable binding process. In addition, the extracellular fluid concentration is assumed to be the same as the arterial plasma concentration except in muscle. Applied to this model were the following assumptions.

(a) Ouabain is localized in the extracellular space (V_e).
(b) Rapid equilibrium between C_v and C_e (ouabain concentration in extracellular space).
(c) C_v is approximated by C_a (slow binding hybrid model; SBH model).
(d) The tissue concentration is composed of the extracellular fluid concentration and the concentration bound to Na,K-ATPase.

The mass balance equations were described as follows:

$$B_{max} = B + C_b \quad (5)$$

$$K_d = k_{off}/k_{on} \quad (6)$$

$$dC_b/dt = k_{on}C_aB - k_{off}C_b$$

$$= k_{off}/K_dC_aB_{max} - (k_{off}/K_dC_a + k_{off})C_b \quad (7)$$

$$V_tC_t = V_e(C_a + C_b) \quad (8)$$

where C_b and B represent the bound and unbound concentration of Na,K-ATPase. C_a is described by Eqs. (4a) and (4b).

This model was not appropriate to fit the data in muscle, because blood perfusion is not enough to allow approximation that the extracellular fluid concentration is the same as C_a. Therefore, a flow model was applied in which the extracellular fluid concentration was defined as C_v (slow binding flow model; SBF model). The mass balance equations were described as follows:

$$dC_v/dt = Q(C_a - C_v)/V_e - k_{on}C_vB_{max} + (k_{on}C_v + k_{off})C_b \quad (9)$$

$$dC_b/dt = k_{off}/K_dC_vB_{max} - (k_{off}/K_dC_v + k_{off})C_b \quad (10)$$

$$V_tC_t = V_e(C_v + C_b) \quad (11)$$

where Q represents the plasma flow rate.

The time courses of $K_{p,vivo}$ were simulated for heart and muscle based on the slow binding model and are shown in Fig. 2.

Fitting by the SB Model. The time course of ouabain concentration in each tissue was fitted using Eqs. (4a)–(11) by MULTI (RUNGE) with the weight of (plasma concentration)$^{-2}$ (12). The Damping Gauss Newton method was used as the algorithm for the nonlinear least-squares method.

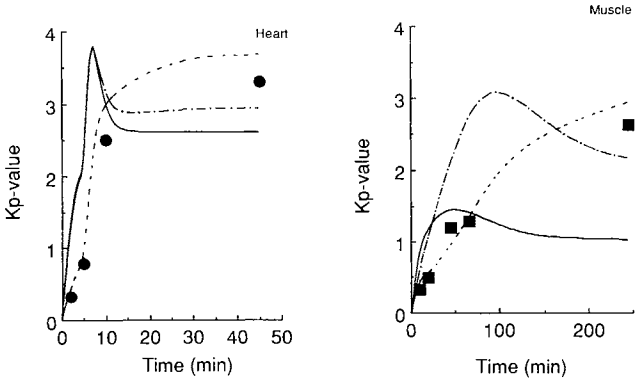

Fig. 2. Time courses of $K_{p,vivo}$ (C_t/C_a) in heart and muscle. $K_{p,vivo}$ was simulated based on the RE model (——), RE model with saturable binding (– · – · –); and SB model (-----). In the RE model, K_p (C_t/C_v) were fixed at 2.5 and 1 for heart and muscle, respectively. The filled circles and squares represent the observed values. The lines represent the calculated $K_{p,vivo}$ based on the models. Parameters used in simulations are described under Methods.

RESULTS

Model Development

The validity of the model was examined by simulating the $K_{p,vivo}$ of heart and muscle based on the RE model and SB model. The result is shown in Fig. 2 with the observed data. In heart, $K_{p,vivo}$ increased rapidly after the termination of infusion (5 min) and then decreased. This overshoot phenomenon in $K_{p,vivo}$ was found in both the linear and the saturable RE model. In muscle, the overshoot was found in both models, although the simulated curves differed between the linear and the saturable RE model. On the other hand, the simulated curves based on the SB model showed no overshoot in both heart and muscle, with a pattern similar to that of the observed data. These simulations rule out the RE model of ouabain tissue concentration time courses.

Fitting by the SB Model

As the initial values for K_d and B_{max}, the results of an *in vitro* binding study (10) were used for each tissue. Literature values were also used as the initial values of the dissociation rate constant (Table I). The results of the curve fittings are shown in Fig. 3. In most tissues, except lung, the concentration increased after the termination of infusion until 10 to 20 min. This pattern was well explained by the SB model. In lung, both observed and calculated concentrations peaked at 5 min. The approximation of C_v by C_a was confirmed by comparing them in each tissue except muscle. In muscle, this approximation was inappropriate, and therefore, the flow model was applied. Thus, the continuous increase in tissue concentration until 20 min could be accounted for. The calculated and observed binding parameters are summarized in Table I. The calculated K_d, B_{max}, and k_{off} agreed well with those of the *in vitro* binding study except muscle. Large differences (10- to 100-fold) were found in muscle between calculated and *in vitro* binding parameters.

Table I. Summary of Binding Parameters from *in Vitro* Binding Experiments and Kinetic Modeling of *in Vivo* Tissue Distribution

	B_{max} (nM)[a]		K_d (nM)		k_{off} (min^{-1})	
Tissue	Obs.[b]	Calc.[c]	Obs.	Calc.	Obs.	Calc.
Heart	5,510	16,800	370	740	0.115[e]	0.0958
	(764)[d]	(3,050)	(82)	(269)		(0.0189)
Muscle	1,970	155	131	1.1	0.156[f]	0.00978
	(739)	(22)	(35)	(1.1)		(0.0129)
Kidney	21,500	13,200	260	280	0.15[f]	0.07088
	(1,600)	(2,690)	(26)	(62)		(0.0707)
Liver	1,350	2,540	415	420		0.0499
	(290)	(5,210)	(150)	(877)		(0.0499)
Lung	1,870	1,820	627	761		0.0603
	(690)	(4,160)	(147)	(1,820)		(0.0343)
Gut	—[g]	1,310	—[g]	39.1		0.0400
		(695)		(34.5)		(0.0145)

[a] B_{max} is calculated based on the assumption that all binding sites are located in the extracellular space as expressed by Eq. (8).
[b] Represents the observed B_{max}, which was calculated from the binding capacity obtained in the 0.5% homogenate (10) times dilution factor, 200, divided by the ratio of V_e/V_t.
[c] Represents the calculated value by the nonlinear least-squares curve fitting of the *in vivo* tissue distribution data by the SB model, using Eqs. (4a)–(11).
[d] Standard deviation in parentheses.
[e] Data from Ref. 4.
[f] Data from Ref. 8.
[g] Binding parameters could not be obtained in gut.

DISCUSSION

An RE model was applied in the construction of a physiological model that accounts for the disposition of many drugs (13–14). In this study, the kinetic analysis was performed on the tissue distribution of ouabain to determine the principal factor in its tissue distribution *in vivo*. The applicability of the RE model was first examined by simulating $K_{p,vivo}$ for heart and muscle. As shown in Fig. 2, a rapid increase and subsequent decrease in $K_{p,vivo}$ were seen in both the linear and the saturable RE model, which differed from the observed results. The observed $K_{p,vivo}$ continued to increase until the end of the study (725 min) in most tissues. The rapid increase in the $K_{p,vivo}$ in the RE model can be explained by the rapid decrease in the plasma concentration of ouabain after the termination of infusion (elimination rate constant at the α phase is 1.06 min^{-1}). The decrease in calculated $K_{p,vivo}$ can be explained by the recovery of the equilibrium between tissue and arterial plasma concentrations (venous plasma concentration is always equilibrated with tissue concentration) in the RE model. After this overshoot phenomenon, the $K_{p,vivo}$ stayed nearly constant and was always higher than K_p (C_t/C_v). The difference depends on the K_p value, blood perfusion rate, tissue volume, and elimination rate constant of the system, as demonstrated by Chen and Gross (15). Since the observed $K_{p,vivo}$ continues to increase, the rapid equilibrium model is inappropriate for the observed tissue distribution time courses.

Active transport of ouabain may occur because of the following observations: (i) Ouabain $K_{p,vivo}$ is greater than one in most tissues (10); (ii) ouabain is hydrophilic and does

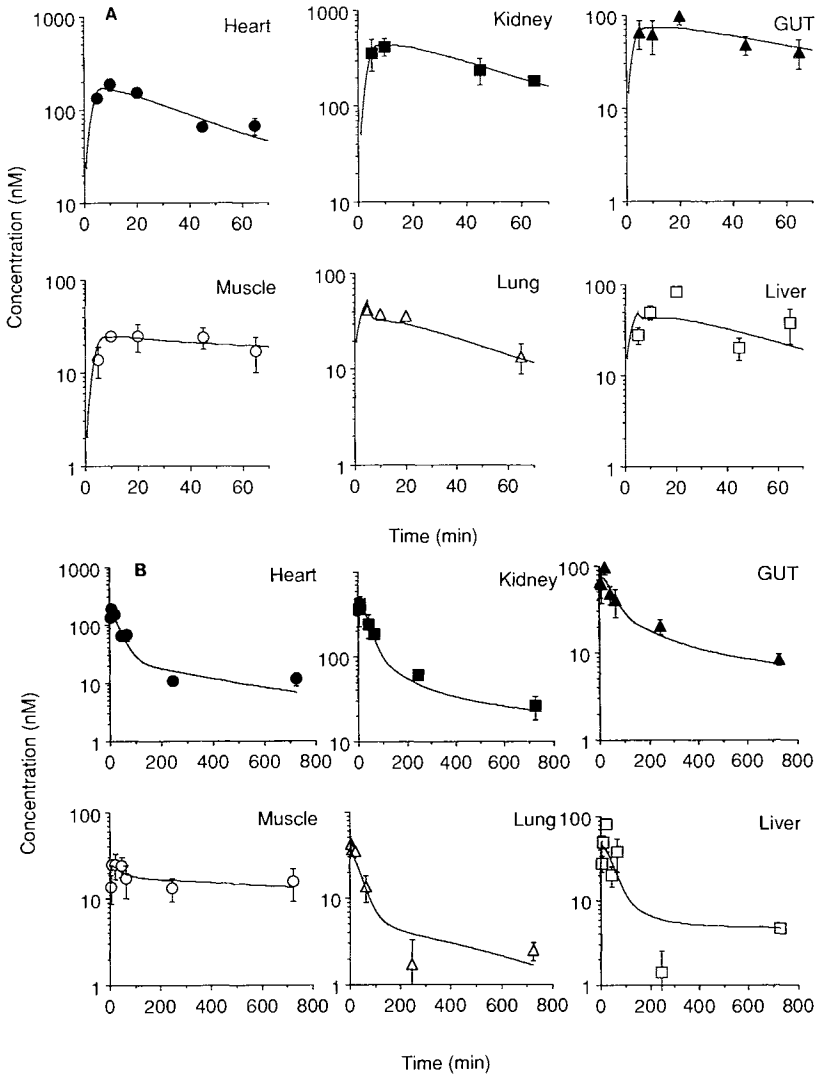

Fig. 3. Time courses of ouabain concentration in each tissue and fitted curve based on the slow binding model. (A) Distribution phase. (B) Elimination phase. Each tissue concentration was measured after the constant infusion of ^{3}H-ouabain at a rate of 10 nmol/min/kg for 5 min. Vertical bar represents standard error (n = 3). (○) Muscle; (●) heart; (■) kidney; (△) lung; (▲) GI; (□) liver.

not penetrate the plasma membrane by simple diffusion (16); and (iii) ouabain binds only to Na,K-ATPase, an enzyme located on the plasma membrane, solely from the extracellular side (17). Therefore binding sites inside the cell can be excluded. Although these observations suggest that ouabain is taken up into the cell by active transport, the binding of ouabain to Na,K-ATPase in *in vitro* experiments excludes this possibility. The correspondence of K_p estimated from the *in vitro* binding experiments, with $K_{p,vivo}$ (9,10) excluded active transport as a major contributor to ouabain tissue distribution.

As shown in Fig. 2, $K_{p,vivo}$ calculated according to the SB model is consistent with the observed data. Therefore, it is reasonable to incorporate slow binding and dissociation processes into the model. We have assumed that C_v is the same as C_a, except in muscle. This approximation was examined by simulating the venous plasma concentration based on the flow model with slow binding between heart and muscle. There was little difference in the calculated C_a and C_v in heart, while the difference was large in muscle (Fig. 4). Although the binding to Na,K-ATPase was extensive in both heart and muscle, the difference between C_a and C_v was small in heart, but large in muscle, especially in the first 5 min. This may result from the difference of perfusion rate per unit volume between muscle and heart. Therefore, a flow model was required to mimic the kinetics of ouabain tissue distribution in muscle.

The SB model curve fitting was successful for most tissues in that the calculated tissue concentration continued to increase after the end of infusion (5 min) until 10 to 20 min. The calculated parameters, those observed in *in vitro* experiments, and the standard deviations are summarized in Table I. For comparison with parameters from the *in vitro* study, the dissociation constant was used instead of the association

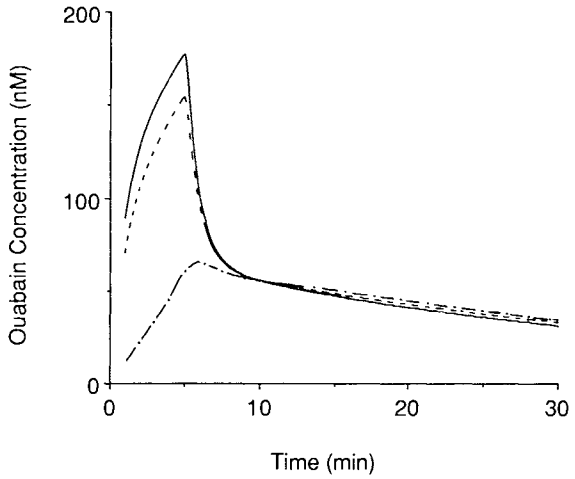

Fig. 4. Comparison of venous plasma concentration between heart and muscle based on the flow model with slow binding process. The C_v were calculated by Eqs. (9)–(11). The binding parameters were fixed at the calculated values shown in Table I. The other parameters are described under Methods. (------) Heart; (– · –) muscle; (——) artery.

rate constant ($K_d = k_{off}/k_{on}$). There was good correspondence between observed and calculated B_{max} and K_d values except in muscle. The binding parameters obtained in *in vitro* experiments are sensitive to the experimental conditions such as potassium concentration (18), and overall correspondence within a few fold is considered reasonable. On the other hand, there was a large difference between observed and calculated parameters in muscle. The decrease in tissue concentration in muscle is much smaller than that in other tissues. The long half-life in muscle was accounted for by the low dissociation constant, which was obtained in the curve fitting. The K_d obtained for muscle is 1.1 n*M*, which is lower than the plasma concentration of ouabain *in vivo* (2–200 n*M*). Thus, saturation could be the reason for the small change of ouabain concentration in muscle.

The dissociation rate constants are summarized in Table I. There is a fairly good correspondence between the calculated and the observed values in heart and kidney, but a 10-fold difference exists in muscle. In this modeling, it was assumed that ouabain can pass the capillary and enter the extracellular space instantaneously in every tissue. In liver, sinusoids have large fenestration with a mean diameter of 200 nm, therefore even albumin can easily enter into the Disse space (19). In the heart, the permeability barrier of the capillary is high and albumin cannot enter the extracellular space during a single passage, but sucrose (MW 342) can (20). Therefore, the permeability barrier may not be important for ouabain (MW 585) in liver and heart. On the contrary, there is a continuous capillary in muscle (21), and there could be a permeability limitation even for ouabain, thereby lowering the apparent dissociation rate constant *in vivo*.

In conclusion, the slow binding process of ouabain to Na,K-ATPase was shown to be important in the tissue distribution of ouabain *in vivo*.

REFERENCES

1. L. I. Harrison and M. Gibaldi. Physiologically based pharmacokinetic model for digoxin distribution and elimination in the rat. *J. Pharm. Sci.* 66:1138–1142 (1977).
2. L. I. Harrison and M. Gibaldi. Physiologically based pharmacokinetic model for digoxin disposition in dogs and its preliminary application to humans. *J. Pharm. Sci.* 66:1679–1683 (1977).
3. O. Hansen. Interaction of cardiac glycosides with ($Na^+ + K^+$)-activated ATPase. A biochemical link to digitalis induced inotropy. *Pharmacol. Rev.* 36:143–163 (1984).
4. D. D. Ku, T. Akera, T. Tobin, and T. M. Brody. Comparative species studies on the effect of monovalent cations and ouabain on cardiac Na^+K^+-adenosine triphosphatase and contractile force. *J. Pharmacol. Exp. Ther.* 197:458–469 (1976).
5. H. Harashima, Y. Sugiyama, Y. Sawada, K. Shigenobu, Y. Kasuya, T. Iga, and M. Hanano. Kinetic analysis of the positive inotropic action (PIA) of ouabain in isolated perfused rabbit heart. Slow onset of PIA and slow binding to Na^+,K^+-adenosine triphosphatase. *J. Pharmacobio-Dyn.* 11:533–540 (1988).
6. T. Tobin and T. M. Brody. Rate of dissociation of enzyme-ouabain complexes and K0.5 values in ($Na^+ + K^+$) adenosine triphosphatase from different species. *Biochem. Pharmacol.* 21:1553–1560 (1972).
7. L. Brown and E. Erdmann. Binding of digitalis derivatives to beef, cat and human cardiac ($Na^+ + K^+$)-ATPase. Affinity and kinetic constants. *Arch. Int. Pharmacodyn.* 271:229–240 (1984).
8. E. Erdmann. Influence of cardiac glycosides on their receptor. In K. Greeff (ed.), *Cardiac Glycosides*, Springer-Verlag, Berlin, 1981, pp. 337–380.
9. H. Harashima, Y. Sugiyama, T. Iga, and M. Hanano. Nonlinear tissue distribution of ouabain in rabbits. *Drug Metab. Disp.* 16:645–649 (1988).
10. H. Harashima, M. Mamiya, M. Yamazaki, Y. Sugiyama, Y. Sawada, T. Iga, and M. Hanano. Significance of binding to Na,K-ATPase in the tissue distribution of ouabain in guinea pigs. *Pharm. Res.* 9:474–479 (1992).
11. A. Tsuji, T. Yoshikawa, K. Nishide, H. Minami, M. Kumura, E. Nakashima, T. Terasaki, E. Miyamoto, C. H. Nighitinale, and T. Yamanaka. Physiologically based pharmacokinetica model for beta-lactam antibiotics. I. Tissue distribution and elimination in rats. *J. Pharm. Sci.* 72:1239–1251 (1983).
12. K. Yamaoka and T. Nakagawa. A nonlinear least squares program based on differential equations, MULTI (LUNGE), for microcomputers. *J. Pharm. Dyn.* 6:595–606 (1983).
13. K. J. Himmelstein and R. J. Lutz. A review of the applications of physiologically based pharmacokinetic modeling. *J. Pharmacokin. Biopharm.* 7:127–145 (1979).
14. L. E. Gerlowski and R. K. Jain. Physiologically based pharmacokinetic modeling: Principles and applications. *J. Pharm. Sci.* 72:1103–1127 (1983).
15. H. S. G. Chen and J. F. Gross. Estimation of tissue-to-plasma partition coefficient used in physiological pharmacokinetic model. *J. Pharmacokin. Biopharm.* 7:117–125 (1979).
16. K. Kuschinsky, H. Lullmann, and P. A. Van Zwieten. A comparison of the accumulation and release of ^{3}H-ouabain and ^{3}H-digitoxin by guinea-pig heart muscle. *Br. J. Pharmacol. Chemother.* 32:598–608 (1968).
17. G. Asano, M. Ashiraf, and A. Schwartz. Localization of Na-K-ATPase in guinea-pig myocardium. *J. Mol. Cell. Cardiol.* 12:257–266 (1980).
18. Y. R. Choi and T. Akera. Kinetic studies on the interaction between ouabain and (Na^+,K^+)-ATPase. *Biochim. Biophys. Acta* 481:648–659 (1977).
19. C. A. Goreski, G. G. Bach, and B. E. Nadeau. On the uptake of material by the intact liver. 52:991–1009 (1973).
20. C. P. Rose, C. A. Goreski, and G. G. Bach. The capillary and sarcolemmal barriers in the heart. *Circ. Res.* 41:515–533 (1977).
21. N. Simionescu and M. Simionescu. The cardiovascular system. In L. Weiss (ed.), *Cell and Tissue Biology*, 6th ed., Urban & Schwarzenberg, Baltimore, MD, 1988, pp. 353–400.